This paper has been published in *Scattering and Surface Roughness III*,
Z.-H. Gu, and A. A. Maradudin, Eds., Proc. SPIE **4100**, 148–155 (2000).

Polarized light scattering measurements of polished and etched steel surfaces

Thomas A. Germer,[a] Thomas Rinder,[b] and Hendrik Rothe[b]

[a]*National Institute of Standards and Technology, Gaithersburg, Maryland 20899*
[b]*University of the Federal Armed Forces, D-22043 Hamburg, Germany*

ABSTRACT

The directional dependence of the intensity and polarization of light scattered by a series of steel surfaces was measured. The samples differ by polishing procedure. Theories for light scattering from microroughness and permittivity variations are reviewed and used to interpret the results. It is shown that the experimental data can be fit to a combination of the two scattering mechanisms, whereby the relative amplitude of the two scattering sources and the complex degree of correlation are treated as adjustable parameters. The fits show a low degree of correlation between the two sources of scatter at low spatial frequencies, with a higher degree of correlation at high spatial frequencies. This correlation has a characteristic phase, common for all of the samples. Comparison of the fitted roughness power spectral density (PSD) functions with those obtained by atomic force microscopy (AFM) showed reasonable but not perfect agreement. This study demonstrates how measurements of the polarization of scattered light can be used to quantify the scatter from two different scattering sources.

Keywords: ellipsometry, optical scatter, permittivity, polarimetry, roughness, steel

1. INTRODUCTION

Light scattering has proven to be a useful method for locating and characterizing defects on a variety of smooth surfaces and for characterizing surface roughness.[1] Recent results have shown that the polarization of scattered light can be used to identify the source of scatter[2–4] and to allow reduction of background noise sources such as roughness.[5] While the intensity of light carries the fluctuations associated with laser speckle, which are directly tied to the randomness of the scattering source, the polarization state of the light does not reflect statistical noise, but rather is a signature of the scattering mechanism. Previous results illustrating these behaviors have been carried out from homogeneous rough surfaces, such as a silicon wafers, optical glasses, or a thick metallic overlayer.[4]

Polarized light scattering not only allows two scattering sources to be distinguished, but allows two coexistent sources to be quantified. Recent measurements have demonstrated that the roughness of two interfaces of a dielectric film can be determined independently using light scattering ellipsometry.[6] The technique is an extension of specular ellipsometry, which is often used to determine film thickness, to the scattering regime, where it can determine film thickness variations or interfacial roughness. The results showed the spatial frequency dependence to the smoothening of the oxide growth interface on silicon.

In this article, we present preliminary results that suggest that the polarization of scattered light can be used to characterize the origin of light scattered by steel with different surface treatments. The two scattering sources considered are roughness of the steel/air interface and inhomogeneity of the steel permittivity. Distinguishing between scatter from these two sources should be useful for assessing and predicting the performance properties of machined surfaces.

In Section 2, we outline vector theories for scattering from roughness and permittivity variations. In Section 3, we describe the scattering ellipsometry technique and the sample preparation. The scattering ellipsometry results will be presented in Section 4. A discussion will follow in Section 5. Finally, in Section 6, the results of this study will be summarized.

2. THEORY

The coordinate system used to describe the incident and scattered light directions and polarizations is outlined in Fig. 1. The *z* axis coincides with the mean surface normal, and light is assumed to be incident at an angle θ_i in the *x*-*z* plane. The direction of scattered light is parameterized by a polar angle θ_r and an azimuthal angle ϕ_r.The right-handed

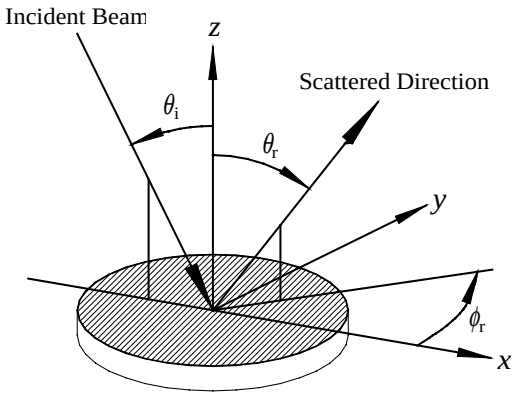

Figure 1. The sample and beam coordinate system.

basis set used to describe the polarization of a plane wave is $\{\hat{\mathbf{s}}, \hat{\mathbf{p}}, \hat{\mathbf{k}}\}$, where $\hat{\mathbf{k}}$ is a unit vector in the direction of propagation, $\hat{\mathbf{s}}$ is a unit vector perpendicular to the plane of incidence (or viewing), and $\hat{\mathbf{p}} = \hat{\mathbf{k}} \times \hat{\mathbf{s}}$ is a unit vector in the plane of incidence (or viewing). There are separate basis sets for the incident and reflected directions, denoted by the subscripts i and r, respectively. The substrate material is assumed to have a complex dielectric constant ε at the wavelength of the incident light, λ. Light which is polarized with its electric field along the $\hat{\mathbf{s}}$ ($\hat{\mathbf{p}}$) direction is considered s-polarized (p-polarized).

Theories for scattering from particulate contaminants and subsurface defects in the Rayleigh limit,[2,7–10] from microtopography,[11] and from small variations in permittivity across the surface[12,13] have been developed elsewhere. In this section, we summarize the results of the theories for scattering from microroughness and subsurface permittivity variations. Each of these theories predicts the form of the Jones scattering matrix,

$$\begin{pmatrix} E_s^{scat} \\ E_p^{scat} \end{pmatrix} = \frac{A \exp(ikR)}{R} \begin{pmatrix} q_{ss} & q_{ps} \\ q_{sp} & q_{pp} \end{pmatrix} \begin{pmatrix} E_s^{inc} \\ E_p^{inc} \end{pmatrix} \tag{1}$$

($k = 2\pi/\lambda$), which relates the components of the scattered electric field $\mathbf{E}^{scat}$ at a distance R from the sample to those of the incident electric field $\mathbf{E}^{inc}$. A harmonic time dependence $\exp(-i\omega t)$ of the fields will be assumed. An overall factor of A, which is common to all four elements of the matrix, does not affect the polarization of the light. Its value is proportional to the 2-d Fourier transform of the surface height profile, in the case of microroughness scattering, and to the 3-d Fourier transform of the permittivity deviation function of the material, in the case of the subsurface permittivity scattering. For comparison with experimental results, the scattering Jones matrix can be converted to its Mueller representation by use of a standard relationship found in the literature.[14–16]

In the smooth-surface limit, where first-order vector perturbation theory (Rayleigh-Rice theory) can be applied, the scattering from microroughness has characteristic Jones matrix elements q_{jk}^{rough}.[11] Scattering from small features below the surface, or from subsurface permittivity variations, results in characteristic Jones matrix elements q_{jk}^{sub}.[12,13] These matrix elements are given by

$$q_{ss}^{rough} = q_{ss}^{sub} = k^2 \cos\phi_r / [(k_{zi} + k'_{zi})(k_{zr} + k'_{zr})], \tag{2a}$$

$$q_{ps}^{rough} = q_{ps}^{sub} = -k'_{zi} k \sin\phi_r / [(\varepsilon k_{zi} + k'_{zi})(k_{zr} + k'_{zr})], \tag{2b}$$

$$q_{sp}^{rough} = q_{sp}^{sub} = -k'_{zr} k \sin\phi_r / [(k_{zi} + k'_{zi})(\varepsilon k_{zr} + k'_{zr})], \tag{2c}$$

$$q_{pp}^{rough} = (\varepsilon k_{xyi} k_{xyr} - k'_{zi} k'_{zr} \cos\phi_r) / [(\varepsilon k_{zi} + k'_{zi})(\varepsilon k_{zr} + k'_{zr})], \tag{2d}$$

$$q_{pp}^{sub} = (k_{xyi} k_{xyr} - k'_{zi} k'_{zr} \cos\phi_r) / [(\varepsilon k_{zi} + k'_{zi})(\varepsilon k_{zr} + k'_{zr})]. \tag{2e}$$

where

$$k_{zj} = k\cos\theta_j ,$$

$$k_{xyj} = k\sin\theta_j ,$$

$$k'_{zj} = k(\varepsilon - \sin^2\theta_j)^{1/2} .$$

The q_{ss}, q_{sp}, and q_{ps} matrix elements are identical for the two scattering mechanisms. Therefore, to differentiate between the two different scattering sources using polarization methods, one must make use of the q_{pp} elements. For example, the incident light can contain some p-polarized light, while the scattered light polarization is measured. Furthermore, since $q_{ps} = 0$ in the plane of incidence for both mechanisms, some s-polarized light must be present to differentiate between the two mechanisms in the plane of incidence or at small scattering angles.

The fields from different sources can add with some degree of coherence, that depends upon the phase correlation between those scattering sources. For two different partial fields, $\mathcal{E}_1$ and $\mathcal{E}_2$, the total intensity is given by [leaving out a factor of the free space impedance, $(\varepsilon_0/\mu_0)^{1/2}$ for brevity]

$$I = \left\langle \left| \mathcal{E}_1 \exp(\mathrm{i}\alpha_1) + \mathcal{E}_2 \exp(\mathrm{i}\alpha_2) \right|^2 \right\rangle , \tag{3}$$

where α_j is the phase associated with the *j*-th partial field, and the average is over any fluctuations that exist in the α_j. With some algebra, Eq. (3) can be rewritten as

$$I = I_1 + I_2 + (I_{12}^{(1)} - I_1 - I_2)\,\mathrm{Re}\,c_{12} + (I_{12}^{(2)} - I_1 - I_2)\,\mathrm{Im}\,c_{12} \tag{4}$$

where $I_j = \left|\mathcal{E}_j\right|^2$ is the intensity of each field alone, $I_{12}^{(1)} = \left|\mathcal{E}_1 + \mathcal{E}_2\right|^2$ is the intensity of the two fields adding coherently in phase, $I_{12}^{(2)} = \left|\mathcal{E}_1 + \mathrm{i}\mathcal{E}_2\right|^2$ is the intensity of the two fields adding coherently but out of phase by $\pi/2$, and $c_{12} = \left\langle \exp[\mathrm{i}(\alpha_1 - \alpha_2)] \right\rangle$ is the degree of phase correlation between the two fields. Eq. (4) also holds when the intensities are interpreted as Stokes vectors or Mueller matrices, where the partial electric fields are treated as Jones vectors or Jones matrices, respectively, and the $|\mathcal{E}|^2$ operation is treated as a conversion from the Jones representation to the Stokes-Mueller representation.

3. EXPERIMENT

3.1. Scattering Ellipsometry

The Goniometric Optical Scatter Instrument (GOSI), which was used to perform the light scattering measurements, is described in detail elsewhere.[17] Briefly, the second harmonic of a cw Nd:YAG laser (λ = 532 nm) was incident onto samples at an angle θ_i, and light scattered into the direction defined by polar angle θ_r and azimuthal angle ϕ_r was collected (see Fig. 1). The polarization state of the incident light was selected with a fixed linear polarizer followed by a rotating $\lambda/2$ linear retarder. The polarization state of the scattered light was analyzed with a rotating $\lambda/4$ linear retarder followed by a fixed linear polarizer.[18] For the measurements shown here, the angles $\theta_i = \theta_r = \theta$ were held fixed and the angle ϕ_r was scanned. In this configuration, the surface spatial frequency being probed, determined by the Bragg relationship, is given by $f = 2\sin\theta\sin(\phi_r/2)/\lambda$. The incident polarization was continuously varied from 45° (p+s) at $\phi_r = 0$, to 90° (p) at $\phi_r = 90°$, and to 135° (p–s) at $\phi_r = 180°$. This incident polarization scheme improves the discrimination between the different scattering mechanisms for all ϕ_r, compared to that using a fixed incident polarization state. For all of the measurements reported in this paper, the incident and scattering angles were $\theta = 60°$.

The intensity and polarization of the scattered light is characterized by the bidirectional reflectance distribution function, f_r, the principal angle of the polarization, η, measured counterclockwise from s-polarization when looking into the direction of propagation, the degree of circular polarization, P_C, and the total degree of polarization, P. These parameters are equivalent to the Stokes parameters, which in a coordinate system rotated by the angle η is

$$\left[f_r,\ f_r(P^2 - P_C^{\ 2})^{1/2},\ 0,\ f_r P_C \right]^T$$

The sign of P_C is chosen to be positive for left-circularly polarized light.

Polarized light scattering measurements were carried out for four different incident azimuthal directions for each sample. The results of these four measurements yield information about how sample non-uniformities contribute to uncertainties in the measurement. Other sources of uncertainty in the scatter measurements are not fully characterized, but are expected to be smaller than the typical point-to-point spacing observed in the data.

3.2. Sample Preparation

Fifteen X5CrNi1810 steel samples, each having diameter 10 mm, were polished with different TiN polishing emulsions (6 μm, 3 μm, 1 μm, 0.25 μm grit sizes) for different times (300 s, 600 s, and 900 s). Three samples polished with 0.25 μm emulsion were further etched in a solution containing 1 % sulfuric acid. Table I outlines the treatment applied and the labeling scheme given to each of the samples.

Table I: Sample preparations

Polishing Time	Polishing Grit Size and Post-Treatment				
	6 μm	3 μm	1 μm	0.25 μm	0.25 μm & etched
300 s	A1	A2	A3	A4	A5
600 s	B1	B2	B3	B4	B5
900 s	C1	C2	C3	C4	C5

Atomic force microscopy (AFM) was performed on each of the fifteen samples. For the purposes of this study, we have converted the images to isotropic 2-d power spectral density (PSD) functions. The isotropic PSDs were obtained by applying 2-d discrete Fourier transforms to the data, and averaging over direction of the resulting 2-d PSDs.

The theories for scattering from roughness and permittivity variations require only the optical constants of the material as parameters. To determine these optical constants, we performed specular ellipsometry measurements at multiple incident angles. The results at different incident angles, however, were not entirely consistent with a two-phase, single interface, model for reflection. Furthermore, the results for each of the samples differed by a small amount. This finding suggests that the samples had some degree of stratification in its surface optical properties. Rather than attempt to modify the light scattering models to account for stratified media, we used the average optical constants determined by specular ellipsometry measurements obtained using the same incident angle as the scattering measurements were performed (60°). The average value (and standard deviations) of the optical constants determined by this procedure was $n = 1.71(0.10)$ and $\kappa = 3.47(0.32)$. The dielectric constant is given by $\varepsilon = (n + i\kappa)^2 = -9.2 + 11.9i$.

4. RESULTS

The samples in each column of Table I behave similarly to each other, which suggests that the polishing time, within the range 300 s to 900 s, does not change the surface morphology by a large amount. To average over statistically insignificant variations in the samples, we averaged the results for Samples A*n*, B*n*, and C*n*, for all four azimuthal orientations of the samples. Figure 2 shows the results of the scattering ellipsometry measurements, and shows the predictions of the two theories describing scattering from surface topography and subsurface permittivity variations. All of the curves begin at small ϕ_r near the predictions of the microroughness model, consistent with the expectation that small angle scattering results from front-surface reflection. For larger ϕ_r, all of the samples show some deviation from the microroughness model. As the scattering angle increases, the results for the parameter η tend towards the subsurface scatter model, yet the results for P_C and P do not necessarily yield such an obvious interpretation.

The curves passing through the data in Fig. 2 represent the results of fitting the data to the roughness and permittivity variation models, allowing the relative intensity of the two models (assuming the lack of scattering from the other mechanism), I_{sub} / I_{rough}, and the complex phase correlation function c_{12} to be adjustable parameters, requiring $|c_{12}| \le 1$.

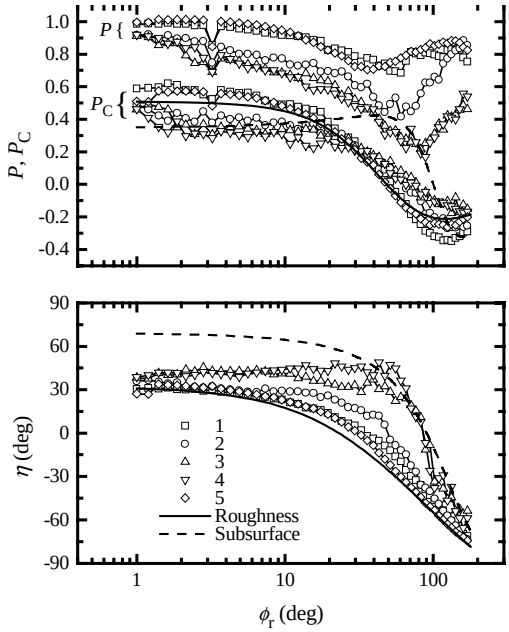

Figure 2. The polarization parameters P, P_C, and η as functions of azimuthal scattering angle. The symbols represent the results of the measurements. The solid curves represent the parameters P_C, and η for scattering from roughness or subsurface permittivity variations alone, for which $P = 1$. The curves passing through the symbols are the results of fits to the data as described in the text.

Since there are three variables describing the polarization, which were fit using three adjustable parameters, excellent fits are nearly always obtained if the choice of mechanisms is appropriate. Such a fit is thus equivalent to an inversion, with no degrees of freedom. The fact that these fits agree well with the data does not assure that we have identified the source of scatter. Figure 3 shows the results for the fitting parameters, plotted versus the spatial frequency of the scattering source, f. The relative intensity at low spatial frequencies approaches zero, as expected, and increases with increasing spatial frequency. The shape of the relative intensity curve is similar for all of the samples, with a slight exception for the etched samples (5).

Figure 4 shows the extracted degree of phase correlation presented on the complex plane. Values near the origin correspond to variations in surface height and material permittivity which exhibit no phase correlation, while those values near the perimeter of the unit circle correspond to high degrees of phase correlation between surface height and material permittivity. The absolute phase of that correlation is determined by the phase of the permittivity variation which corresponds to maxima or minima in the surface height function. When there is a high degree of correlation, the absolute phase would be expected to be related to the difference in the dielectric function of the softer parts of the steel versus that of the harder parts. Most of the results are quite scattered about the center of this plot, suggesting lack of much correlation between the two scattering sources. At low spatial frequencies, Samples 1 displayed results that extended out a radial labeled A on Fig. 4. The angle of this radial was very dependent upon details of the fitting procedure, such as the index of refraction used for the material. Since the signals observed from the sample at these angles were dominated by roughness scattering, we do not believe that the correlation function of these points is significant. However, for higher spatial frequencies, where the correlation function can be seen to increase, all of the samples show correlation functions extending out along a single radial (labeled B in Fig. 4). Compositional variations in the steel alloy would be expected to affect both the optical properties of the material and its physical properties, such as hardness. These results suggest that the roughness profile of the material at higher spatial frequencies is correlated to changes in the material properties.

The fits to the two mechanisms yield the PSD of the surface roughness function and the PSD of the permittivity variations on the surface. Figure 5 shows the results of the roughness PSD for all five sets of samples, compared to those measured by AFM. The agreement between the scattering results and the AFM measurements is reasonable but not perfect.

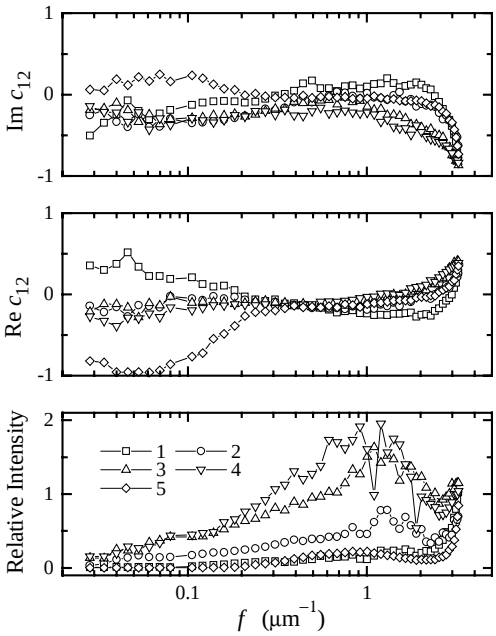

Figure 3. Results of relative amplitude and cross correlation parameters obtained from fitting Eq. (4) to the polarized light scattering data.

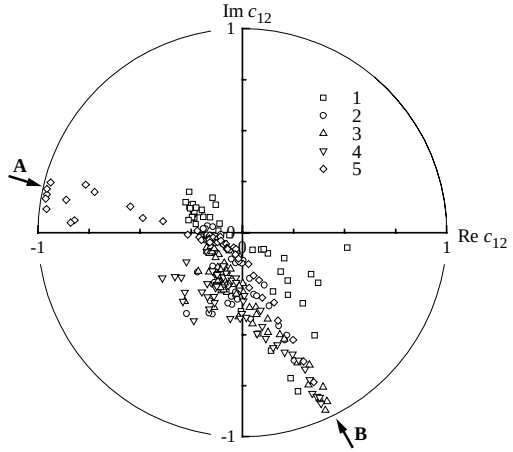

Figure 4. The phase correlation function c_{12} shown on the complex plane. The two arrows (A and B) point to radials discussed in the text.

5. DISCUSSION

We must be emphasize that these results represent those of a preliminary study and are highly speculative in nature. The technique of scattering ellipsometry has not been fully established as a method for distinguishing amongst different scattering sources, and we have not carried out a full characterization of the uncertainties that result from the analysis. Evaluating some of these uncertainties is difficult. For example, the lack of a consistent measurement of the optical constants of the samples suggests that the samples have some degree of stratification, a finding which is not accounted for by the light scattering models. Therefore, this study represents a piece in a puzzle that may eventually yield the ability for light scattering ellipsometry to quantify the levels of two different scattering sources.

The results presented above, however, show consistencies, which indicate that the findings have some truth to them. For example, the correlation function shown in Fig. 4 behave as one would expect. That is, at certain spatial

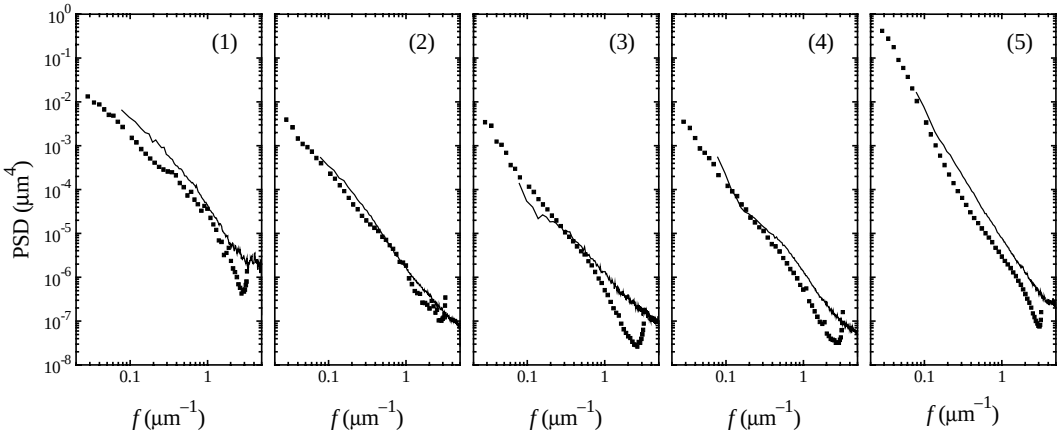

Figure 5. Comparison of between the results of the PSD function of the surface roughness obtained from the scatter measurements (symbols) with those obtained from AFM measurements (curves).

frequencies, the height variations are uncorrelated with the material variations, while at others they are highly correlated. Those scattering directions for which the data are correlated are consistent between all of the samples and extend as a line from the origin outward. Less consistent is the comparison between the surface height PSDs obtained by the light scattering and those obtained by AFM.

The use of light scattering to characterize roughness must be treated with some care. In the past, it has been difficult to critically assess if scatter resulted from topography. The most common method for this determination was to perform wavelength-scaling measurements, that is, comparing the results of analyses carried out at multiple wavelengths.[1] However, scattering from very small subsurface defects show very similar scaling behaviors to that of microroughness.[2] Subsurface permittivity variation is expected to show large wavelength dispersion, which results in its not typically following wavelength scaling behaviors. The polarization, however, is a unique signature of the scattering mechanism, and for microroughness is quite rigorous.

6. SUMMARY

Polarized light scattering measurements were performed on steel samples polished and etched to varying degrees. The theories for light scattering from microroughness and permittivity variations were presented and used to interpret the data. The results demonstrate that the light scattering from these materials cannot be classified as coming from a single source, and the relative amounts of the two scattering sources depends upon scattering direction and sample preparation. The results are consistent with scattering resulting from a combination of roughness and subsurface permittivity variations.

REFERENCES AND NOTES

1. J. C. Stover, *Optical Scattering: Measurement and Analysis*, (SPIE Optical Engineering Press, Bellingham, WA, 1995).

2. T. A. Germer, "Angular dependence and polarization of out-of-plane optical scattering from particulate contamination, subsurface defects, and surface microroughness," Appl. Opt. **36,** 8798-8805 (1997).

3. T. A. Germer, C. C. Asmail, and B. W. Scheer, "Polarization of out-of-plane scattering from microrough silicon," Opt. Lett. **22,** 1284-1286 (1997).

4. T. A. Germer and C. C. Asmail, "Polarization of light scattered by microrough surfaces and subsurface defects," J. Opt. Soc. Am. A **16,** 1326-1332 (1999).

5. T. A. Germer and C. C. Asmail, "Microroughness-blind hemispherical optical scatter instrument," United States Patent #6,034,776 (Mar. 7, 2000).

6. T. A. Germer, "Measurement of roughness of two interfaces of a dielectric film by scattering ellipsometry," Phys. Rev. Lett. in press (2000).

7. G. Videen, "Light scattering from a sphere on or near a surface," J. Opt. Soc. Am. A **8,** 483-489 (1991).

8. G. Videen, W. L. Wolfe, and W. S. Bickel, "Light scattering Mueller matrix for a surface contaminated by a single particle in the Rayleigh limit," Opt. Eng. **31,** 341-349 (1992).

9. G. Videen, M. G. Turner, V. J. Iafelice, W. S. Bickel, and W. L. Wolfe, "Scattering from a small sphere near a surface," J. Opt. Soc. Am. A **10,** 118-126 (1993).

10. G. Videen, "Light scattering from a sphere behind a surface," J. Opt. Soc. Am. A **10,** 110-117 (1993).

11. D. E. Barrick, "Rough Surfaces," in *Radar Cross Section Handbook* (Plenum, New York, 1970) Chap. 9.

12. J. M. Elson, "Theory of light scattering from a rough surface with an inhomogeneous dielectric permittivity," Phys. Rev. B **30,** 5460-5480 (1984).

13. J. M. Elson, "Characteristics of far-field scattering by means of surface roughness and variations in subsurface permittivity," Waves in Random Media **7,** 303-317 (1997).

14. C. F. Bohren and D. R. Huffman, *Absorption and Scattering of Light by Small Particles*, (Wiley, New York, 1983).

15. H. C. van de Hulst, *Light Scattering by Small Particles*, (Dover, New York, 1981).

16. D. S. Flynn and C. Alexander, "Polarized surface scattering expressed in terms of a bidirectional reflectance distribution function matrix," Opt. Eng. **34,** 1646-1650 (1995).

17. T. A. Germer and C. C. Asmail, "Goniometric optical scatter instrument for out-of-plane ellipsometry measurements," Rev. Sci. Instr. **70,** 3688-3695 (1999).

18. R. A. Chipman, "Polarimetry," in *Handbook of Optics II* (McGraw-Hill, New York, 1995) Chap. 22.